Cancer Research

CDK2 Inhibition Causes Anaphase Catastrophe in Lung Cancer through the Centrosomal Protein CP110

Shanhu Hu[1,5], Alexey V. Danilov[2,4,5], Kristina Godek[3,4,5], Bernardo Orr[3,4,5], Laura J. Tafe[5,6], Jaime Rodriguez-Canales[7], Carmen Behrens[7], Barbara Mino[7], Cesar A. Moran[8], Vincent A. Memoli[4,5,6], Lisa Maria Mustachio[1,5], Fabrizio Galimberti[1,5], Saranya Ravi[1,5], Andrew DeCastro[1,5], Yun Lu[1,5], David Sekula[1,5], Angeline S. Andrew[4,5,9], Ignacio I. Wistuba[7], Sarah Freemantle[1,5], Duane A. Compton[3,4,5], and Ethan Dmitrovsky[1,2,4,5]

Abstract

Aneuploidy is frequently detected in human cancers and is implicated in carcinogenesis. Pharmacologic targeting of aneuploidy is an attractive therapeutic strategy, as this would preferentially eliminate malignant over normal cells. We previously discovered that CDK2 inhibition causes lung cancer cells with more than two centrosomes to undergo multipolar cell division leading to apoptosis, defined as anaphase catastrophe. Cells with activating *KRAS* mutations were especially sensitive to CDK2 inhibition. Mechanisms of CDK2-mediated anaphase catastrophe and how activated *KRAS* enhances this effect were investigated. Live-cell imaging provided direct evidence that following CDK2 inhibition, lung cancer cells develop multipolar anaphase and undergo multipolar cell division with the resulting progeny apoptotic. The siRNA-mediated repression of the CDK2 target and centrosome protein CP110 induced anaphase catastrophe of lung cancer cells. In contrast, CP110 overexpression antagonized CDK2 inhibitor–mediated anaphase catastrophe. Furthermore, activated *KRAS* mutations sensitized lung cancer cells to CDK2 inhibition by deregulating CP110 expression. Thus, CP110 is a critical mediator of CDK2 inhibition–driven anaphase catastrophe. Independent examination of murine and human paired normal–malignant lung tissues revealed marked upregulation of CP110 in malignant versus normal lung. Human lung cancers with *KRAS* mutations had significantly lower CP110 expression as compared with *KRAS* wild-type cancers. Thus, a direct link was found between CP110 and CDK2 inhibitor antineoplastic response. CP110 plays a mechanistic role in response of lung cancer cells to CDK2 inhibition, especially in the presence of activated *KRAS* mutations. *Cancer Res; 75(10); 2029–38. ©2015 AACR.*

Introduction

Cyclin-dependent kinases (CDK) regulate cell-cycle progression (1). CDK2 is activated by the temporal upregulation of cyclin E promoting DNA duplication, entry, and progression through the cell cycle (2). Cyclin E-CDK2 deregulation is frequent in epithelial carcinogenesis, including in lung cancer, where it is associated with a poor prognosis (3). Transgenic mouse models were engineered with surfactant C-targeted cyclin E expression in the lung (4). This conferred chromosomal instability and lung cancers in mice with tumors recapitulating key features of human lung carcinogenesis (4).

Our prior work reported CDK2 inhibition caused anaphase catastrophe and apoptosis in lung cancer cells (5). Results from a high-throughput screen system testing the effect of seliciclib in 270 cancer cell lines revealed that in non–small cell lung cancer (NSCLC) cell lines, the most sensitive lines frequently had activated *KRAS*, whereas the 15 least sensitive cell lines all had wild-type (WT) KRAS, indicating that *KRAS*-mutant lung cancer cell lines are most sensitive to CDK2 inhibition (5). Notably, lung cancer cases with activated *KRAS* are chemoresistant and have a poor prognosis (6). Therapeutic strategies for lung cancers with *KRAS* mutations are needed. This study sought to elucidate mechanistic pathways through which CDK2 inhibition confers anaphase catastrophe, and how *KRAS* mutation enhances this effect.

Anaphase catastrophe is observed in cancers with extra centrosomes that segregate chromosomes with multipolar spindles into nonviable cells (7, 8). Centrosome amplification occurs in diverse cancers and is associated with chromosome instability, anaphase

[1]Department of Pharmacology and Toxicology, Geisel School of Medicine at Dartmouth, Hanover, New Hampshire. [2]Department of Medicine, Geisel School of Medicine at Dartmouth, Hanover, New Hampshire. [3]Department of Biochemistry, Geisel School of Medicine at Dartmouth, Hanover, New Hampshire. [4]The Norris Cotton Cancer Center, Geisel School of Medicine at Dartmouth, Hanover, New Hampshire. [5]Dartmouth-Hitchcock Medical Center, Lebanon, New Hampshire. [6]Department of Pathology, Geisel School of Medicine at Dartmouth, Hanover, New Hampshire. [7]Department of Translational Molecular Pathology, The University of Texas MD Anderson Cancer Center, Houston, Texas. [8]Department of Pathology, The University of Texas MD Anderson Cancer Center, Houston, Texas. [9]Department of Community and Family Medicine, Geisel School of Medicine at Dartmouth, Hanover, New Hampshire.

Note: Supplementary data for this article are available at Cancer Research Online (http://cancerres.aacrjournals.org/).

Current address for Ethan Dmitrovsky: Departments of Thoracic and Head and Neck Medical Oncology, Division of Cancer Medicine, The University of Texas MD Anderson Cancer Center, Houston, TX.

Corresponding Author: Ethan Dmitrovsky, Geisel School of Medicine at Dartmouth, HB7650, Hanover, NH 03755. Phone: 603-650-1667; Fax: 603-650-1129; E-mail: ethan.dmitrovsky@dartmouth.edu

doi: 10.1158/0008-5472.CAN-14-1494

catastrophe, aneuploidy, and tumorigenesis (9–13). Agents that cause anaphase catastrophe, including CDK2 inhibitors, exploit the fact that cancer cells with supernumerary centrosomes can undergo multipolar cell division, leading to aneuploidy and cell death (14).

To identify potential mediators of anaphase catastrophe engaged by CDK2 inhibition, several CDK2 targets were examined. Among them, the centrosomal protein CP110 was highlighted as CP110 knockdown increased anaphase catastrophe in lung cancer cells. CP110 is a direct target of cyclin E-CDK2, cyclin A-CDK2, and cyclin B-CDC2 (15). CP110 has differing roles dependent on cell-cycle phase (15–20). During the G_1–S phase, CP110 regulates centrosome duplication and maturation (15, 16), and during the M phase it is involved in cytokinesis (17). In noncycling cells and cells in G_0 phase, CP110 inhibits primary cilia formation (18, 19). CP110 knockdown prevents centrosome reduplication in S-phase–arrested cells and induces premature centrosome separation (15), resulting in tetraploidy and binucleate cells, indicating cytokinesis failure (17).

This study demonstrates in lung cancer cells that CDK2 inhibition causes multipolar anaphase that temporally precedes apoptosis and cell death. We found that CP110 is a mediator of CDK2 inhibitor–conferred anaphase catastrophe. Intriguingly, *KRAS* mutations sensitized lung cancers to CDK2 inhibitor–mediated anaphase catastrophe by deregulating CP110 expression. Translational relevance of these CP110 findings was established by comprehensively examining human malignant lung tissue arrays with an associated clinical database and by investigating lung cancers from engineered mouse models. Findings presented here reveal a direct role for CP110 in lung cancer response to CDK2 inhibition, especially when *KRAS* mutations were detected.

Materials and Methods

Chemicals and antibodies

Seliciclib (CYC202, R-roscovitine) was provided by Cyclacel (stock solution 10 mmol/L in DMSO). Dosages of seliciclib used in the study (5, 10, and 15μmol/L) are clinically achievable (21), and biologic effects of seliciclib at those dosages were due to CDK2 inhibition rather than to CDK7/9 blockade (5). Antibodies used were: cytochrome C (556432; BD Pharmingen. 1:1,000), α-tubulin (T6199; Sigma-Aldrich. 1:10,000), CP110 (sc-136629; Santa Cruz Biotechnology, Inc.; 1:1,000), actin (sc-1615; Santa Cruz Biotechnology, Inc.; 1:3,000), *KRAS* (sc-30; Santa Cruz Biotechnology, Inc.; 1:1,000), Texas Red anti-mouse IgG (H+L; TI-2000, Vector Laboratories, Inc.), ECL anti-rabbit lgG (NA934V, GE Healthcare), ECL anti-mouse lgG (NA931V; GE Healthcare), and horseradish peroxidase–conjugated donkey anti-goat IgG (sc-2020; Santa Cruz Biotechnology, Inc.). Pro-Long Gold anti-fade reagent with 4′,6-diamidino-2-phenylindole (DAPI; P36935; Invitrogen) preserved immunofluorescence.

Cell culture

The murine lung cancer cell line ED-1 was derived and cultured, as described previously (22). LKR13, 344p, and 393p murine lung cancer cell lines were provided by others (23). Human lung cancer cell lines Hop62, A549, H460, and H522 were purchased from the ATCC and cultured as described previously (22).

Live-cell imaging

Cells plated on coverslips were treated with seliciclib (15 μmol/L) or vehicle for 24 hours before live-cell imaging. Multipolar metaphase cells were individually selected for time-lapse live-cell imaging, as described previously (8). DIC images were acquired with a Nikon Eclipse Ti microscope and an Andor cooled CCD camera using a 60 × 1.4NA oil immersion objective. For Hop62 cell imaging, 21 *z*-axis optical sections of 0.5 μm were acquired at 10 minutes intervals for 25 hours.

Following time-lapse imaging, cells were fixed with 3.5% paraformaldehyde and stained with DAPI and a cytochrome C-specific antibody. Fluorescent images were acquired using 11 *z*-axis optical sections of 1.0 μm. Image stacks and full-volume renderings were performed using Nikon Elements and contrast enhancement was aided by Adobe Photoshop software. Cytochrome C immunofluorescence images were quantified by calculating average (mean) of the mean pixel intensity of at least 20 regions of interest (area = 0.8 μm^2) within each cell to avoid any mitochondrial staining and quantify only cytoplasmic cytochrome C. Background levels for each image were subtracted.

Expression plasmids and transient transfection

HA-tagged WT pcDEF3-CP110 (CP110-WT) vector and a CP110 vector with 8 phosphorylation sites mutated pcDEF3-CP110 (CP110-MUT) were generous gifts from others (15). Logarithmically growing ED-1, LKR13, Hop62, H522, A549, and H460 cell lines were each transiently transfected using TransIT-LT1 reagent (Mirus), following the manufacturer's instructions. Each experiment was independently replicated at least three times.

Indicated lung cancer cells were transfected with siRNAs using Lipofectamine 2000 (Invitrogen). The siRNAs targeting murine CP110 (Dharmacon), human or murine CDK2 (IDT) and human or murine KRAS (Thermo Fisher Scientific) species and RISC control siRNA (Dharmacon, IDT and Thermo Fisher Scientific) were purchased and validated for effects of each knockdown by immunblot and qPCR assays. siRNA sequences appear in Supplementary File. S1. Each experiment was independently replicated at least three times.

Multipolar anaphase assay

Indicated lung cancer cells were fixed in cold methanol and stained with DAPI and an anti–α-tubulin–specific antibody and examined using an Eclipse TE 2000-E microscope (Nikon). Anaphase cells that contained three or more spindle poles were scored as multipolar. Data were expressed as the percentage of multipolar versus total anaphase cells.

Generation of stable *KRAS* transfectants

Logarithmically growing ED-1 cells (3×10^6) were plated in each 10-cm tissue culture dish, 24 hours before transfection. Twelve μg each of the pCGN K-$Ras^{G12V,\ 188L}$ plasmid (Addgene) with the pPUR expression plasmid (Clontech) or an empty vector with the pPUR plasmid was individually transfected into ED-1 cells using Lipofectamine 2000 (Invitrogen). Puromycin selection began 24 hours after transfection. Engineered *KRAS* overexpression was confirmed by immunoblot analysis.

Proliferation and apoptosis assays

Logarithmically growing cells were plated onto individual 12-well tissue culture plates (5×10^3 cells/well). Twenty-four hours later, cells were treated with seliciclib over a range of concentrations versus vehicle controls. Three independent wells were

seeded in each experiment with triplicate independent replicates. Proliferation was measured using the CellTiter-Glo Assay Kit (Promega), as described previously (24). Trypan blue viability assays were performed (22). Cellular apoptosis was measured by Annexin V:PE positivity detected using the Annexin V Assay Kit (Southern Biotech).

Immunohistochemistry

Thirty lung cancers (17 adenocarcinoma, eight squamous cell, and five other histologies) from the New Hampshire State Cancer Registry and Dartmouth Tumor Registry in addition to lung cancer specimens obtained from Dartmouth's Department of Pathology archives were used in paired normal and malignant lung tissue microarrays. This study was reviewed and approved by the Dartmouth Committee for Protection of Human Subjects.

A larger set of tissue microarrays was from a lung cancer tissue bank at the MD Anderson Cancer Center. The Institutional Review Board approved these studies of 558 surgically resected NSCLC (369 adenocarcinomas, 176 squamous cell carcinomas, 13 histology information not available).

IHC was performed on formalin-fixed paraffin-embedded sections using a Leica BOND-MAX automated stainer (Leica Microsystems Inc.) and Leica Bond Polymer Refine Detection reagents to detect CP110 protein. Antibody specificity was confirmed using a blocking peptide (sc-136629; Santa Cruz Biotechnology Inc.). The IHC scoring system was similar to prior work (22, 25). CP110 immunohistochemical expression was scored by a reference pathologist who was unaware of clinical findings. Both average staining intensity and percentages of immunoreactive cancer cells were recorded.

CP110 imunohistochemical analyses were independently performed in paired normal–malignant lung tissues from cyclin E as well as *KRAS*-driven lung cancers in engineered mouse models (4, 26).

Immunoblot analyses

Cells were lysed with ice-cold RIPA buffer with protease inhibitors (BD Biosciences), and immunoblot analyses performed as previously described (27). Lysates were size-fractionated by SDS-PAGE before transfer to nitrocellulose membranes (Schleicher and Schuell Bioscience) and probing with indicated antibodies.

Real-time reverse transcription PCR assays

Total RNA was isolated from cells using the RNA Easy Kit (Invitrogen). Reverse transcription (RT) was done using the High Capacity cDNA Reverse Transcription Kit (Applied Biosystems) with a Peltier Thermal Cycler (MJ Research). Quantitative real-time PCR assays were done using SYBR Green PCR Master Mix (Applied Biosystems) and the 7500 Fast Real time PCR System (Applied Biosystems) for quantitation. RT-PCR assays were conducted following the manufacturer's protocol (Applied Biosystems). Three replicate experiments were done. Primers sequences appear in Supplementary File S1.

Statistical analyses

Results of independent experiments were pooled to assess statistical significance. Two-tailed *t* tests were used. Statistical significance was noted with *, $P < 0.05$ and **, $P < 0.01$.

Results

Live-cell imaging after CDK2 inhibition

Prior work established CDK2 inhibition caused anaphase catastrophe in lung cancer cells (5, 7). Although prior work revealed most progeny of multipolar cell divisions died or arrested regardless of cell origin (8), direct evidence linking anaphase catastrophe with induced cell death after CDK2 inhibition in lung cancer cells remained to be shown. To determine the outcomes of cells undergoing multipolar anaphase, we used live-cell imaging to follow their fates following CDK2 inhibitor treatment. A representative Hop62 human lung cancer cell displaying a multipolar metaphase was selected by DIC imaging and followed by time lapse microscopy. After 25 hours of imaging (Fig. 1A, whole video is provided in Supplementary File S2), Hop62 cells were fixed and stained for cytochrome C and DAPI. Cytoplasmic cytochrome C was quantified in progeny. In Fig. 1B, representative negative and positive control cells appear in the examined field. Compared with these cells, two of the daughter cells had significant cytoplasmic cytochrome C release, as quantified in Fig. 1C, indicating apoptosis was initiated. The third daughter cell did not show a significant cytoplasmic cytochrome C signal. However, the third daughter cell displayed marked DNA fragmentation and micronuclei, features seen before cell death or senescence (28). These results provide direct evidence that progeny of lung cancer cells undergoing multipolar anaphases can undergo apoptosis.

CP110 regulates anaphase catastrophe

Because CP110 regulates centrosome function and is a direct CDK2 phosphorylation target (15), it was hypothesized CDK2 inhibition induced anaphase catastrophe via CP110. To investigate whether CP110 knockdown caused anaphase catastrophe, two different siRNAs targeting murine CP110 and a scrambled control siRNA were each used. Real-time quantitative RT-PCR assays validated knockdown of targeted mRNAs. Marked knockdown of CP110 mRNA was achieved at both 24 and 48 hours following transfection (Fig. 2A, left). CP110 knockdown significantly increased percentages of cells undergoing multipolar anaphase in murine ED-1 lung cancer cells; overexpression of WT CP110 abrogated anaphase catastrophe conferred by CP110 knockdown (Fig. 2A, middle).

To investigate whether CP110 knockdown augmented anaphase catastrophe by selicicib-mediated CDK2 inhibition, CP110-depleted ED-1 murine lung cancer cells were treated with seliciclib for 24 hours and scored for multipolar anaphase (Fig. 2A, right). CP110 knockdown increased multipolar anaphases induced by seliciclib treatment in ED-1 cells.

To examine whether increased CP110 levels affected anaphase catastrophe via CDK2 inhibition, CDK2 activity was repressed, genetically or pharmacologically, and CP110 was simultaneously overexpressed in ED-1 cells (Fig. 2B). CP110 overexpression was confirmed by immunoblot analyses (Supplementary Fig. S1A) and CDK2 knockdown was validated by real-time quantitative RT-PCR assays and immunoblot analyses (Fig. 2B, left). Overexpression of CP110 significantly antagonized multipolar anaphases induced by either Cdk2 knockdown (Fig. 2B, middle) or seliciclib treatment (Fig. 2B, right). CP110 overexpression also significantly reduced apoptosis caused by seliciclib treatment (Supplementary Fig. S1B).

To examine whether seliciclib treatment affected CP110 expression level, we examined basal levels of CP110 at 24 and 48 hours

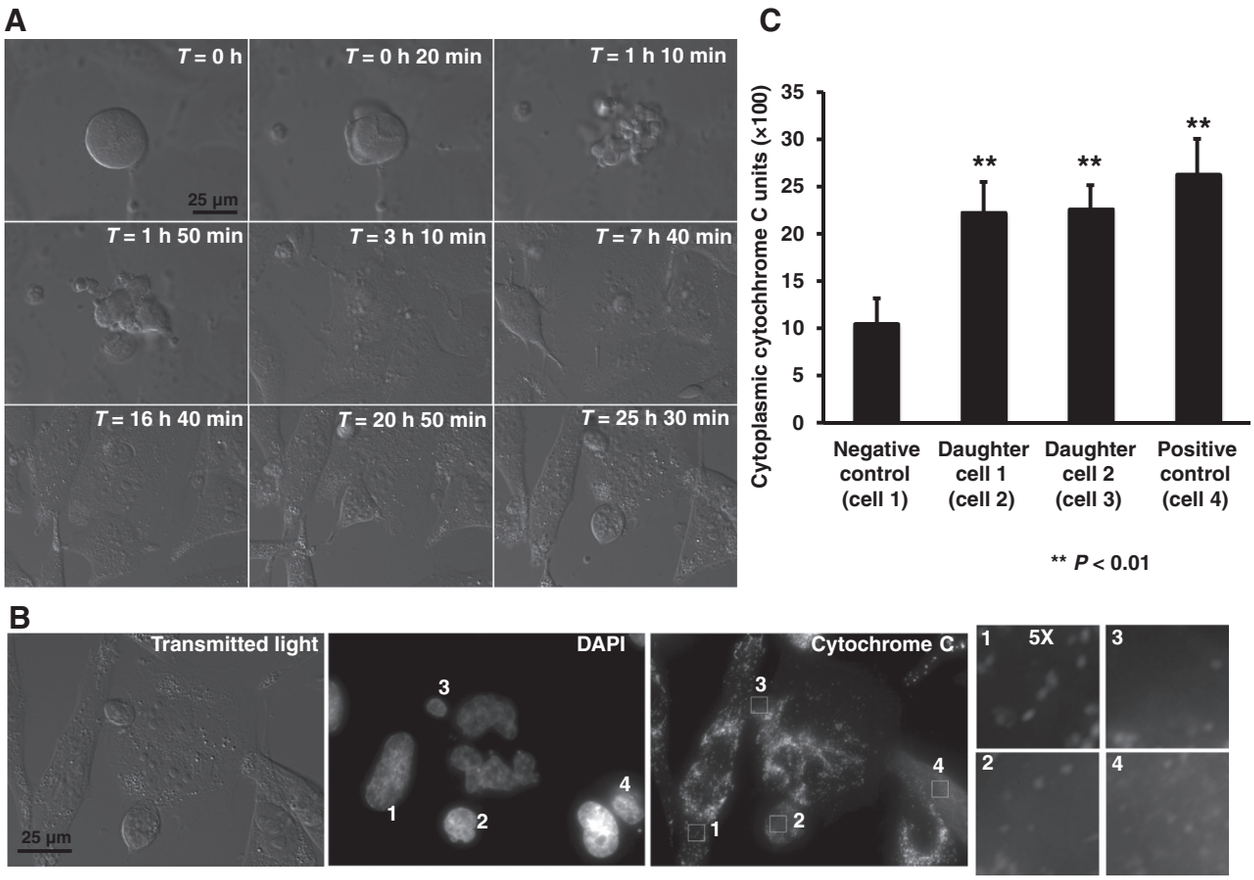

Figure 1.
Live-cell imaging revealed the fate of cells undergoing multipolar anaphase. A, a representative Hop62 multipolar metaphase cell was selected and filmed for 25 hours. Hop62 cells were treated with seliciclib (15 μmol/L) for 24 hours before filming and were in medium with seliciclib (15 μmol/L) during filming. B, Hop62 cells filmed in A were fixed and stained for cytochrome C and DAPI. The signals of cytoplasmic cytochrome C of daughter cells as displayed were enlarged. C, the quantification of cytoplasmic cytochrome C in each progeny is shown.

after seliciclib treatment. Treatment of seliclcib did not appreciably affect CP110 protein levels in human and murine lung cancer cells (Supplementary Fig. S1E).

To investigate whether CP110 phosphorylation was critical for protecting cells from undergoing anaphase catastrophe induced by CDK2 inhibition, a mutant CP110 species with all potential CDK2 phosphorylation sites transversed to alanines (15) was transfected into murine lung cancer cells. Mutant CP110 overexpression did not antagonize induction of multipolar anaphase (Supplementary Fig. S1C) or apoptosis (Supplementary Fig. S1D) in ED-1 cells treated with the CKD2 inhibitor seliciclib. Similar results were observed in LKR13 murine lung cancer cells (Supplementary Fig. S2) and A549 human lung cancer cells (data not shown). Together, these studies indicated that increasing WT CP110 protein could override CDK2 inhibition and protect cells from anaphase catastrophe. Cells with lower CP110 levels are particularly sensitive to CDK2 inhibition.

The working model hypothesized that inhibition of CDK2 decreases CP110 phosphorylation levels, which leads to anaphase catastrophe. Moreover, activated KRAS can downregulate CP110 basal levels, increase lung cancer cellular response to CDK2 inhibitors (Schematic diagram in Supplementary Fig. S3A).

Engineered CP110 overexpression in human lung cancer cells

To investigate whether CP110 overexpression can rescue anaphase catastrophe caused by CDK2 inhibition in human lung cancer cells, A549, Hop62, H460, and H522 cells were each engineered with CP110 overexpression (Supplementary Fig. S3B) before seliciclib treatment (15 μmol/L) for 4, 8, and 24 hours. Induction of multipolar anaphases by CDK2 inhibition was observed as early as 4 hours after drug treatment of all four cell lines (Fig. 3A), whereas apoptosis induction did not occur until 24 hours of this treatment (Fig. 3B). CDK2 knockdown was achieved by independent siRNAs following CP110 overexpression in A549 and Hop62 cell lines. Real-time quantitative RT-PCR assays validated CDK2 knockdown (Fig. 4A and 4B, left) and multipolar anaphases were scored 24 hours after transfection (Fig. 4A and B, right). Consistent with results from murine cells, engineered CP110 overexpression substantially reduced multipolar anaphases and apoptosis in all examined human lung cancer cell lines, despite seliciclib treatment or CDK2 knockdown. Engineered gain of WT CP110 expression protected both human and murine lung cancer cell lines from undergoing anaphase catastrophe and apoptosis induced by pharmacologic inhibition or genetic knockdown of CDK2.

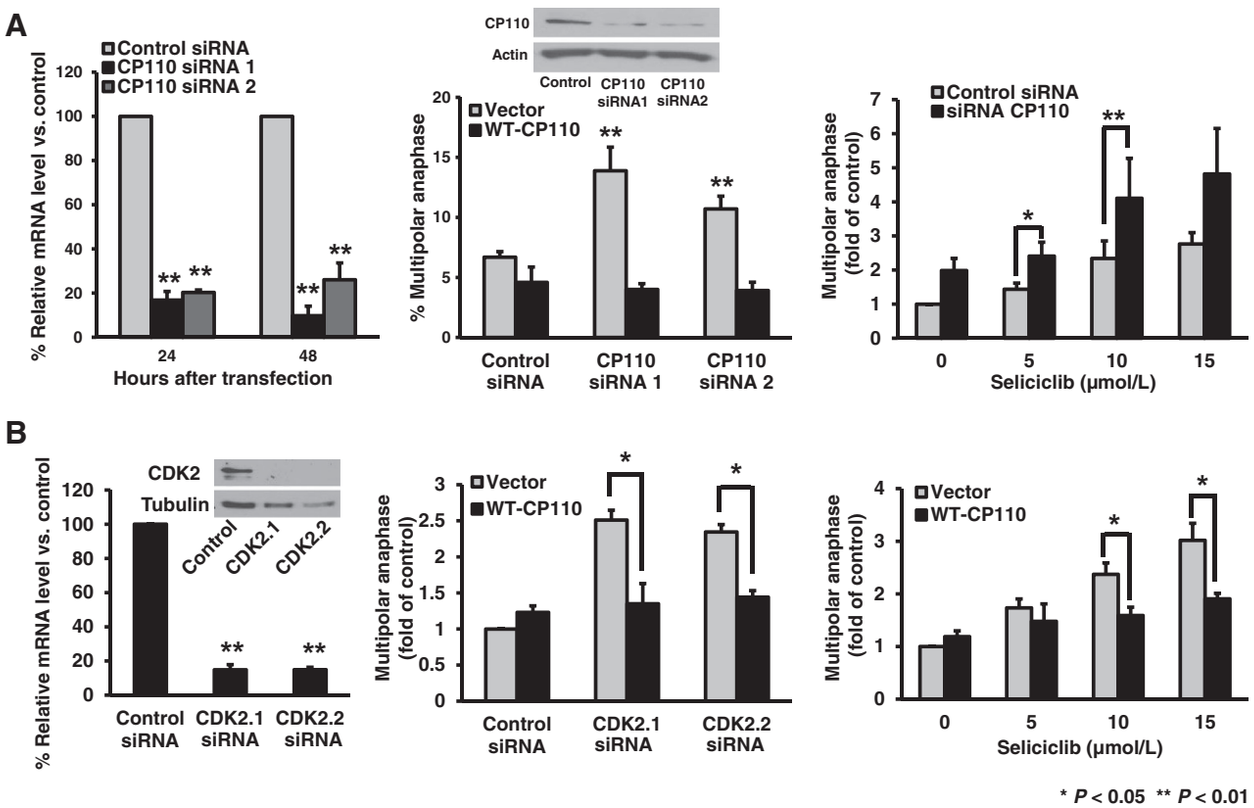

Figure 2.
Gain or loss of CP110 function in murine lung cancer cells implicates it in CDK2 inhibition–mediated anaphase catastrophe. A, effect of knockdown CP110 on anaphase catastrophe. Left, confirmation of CP110 mRNA knockdown by real-time RT-PCR assays performed 24 and 48 hours after transfection. Immunoblot confirmation of CP110 knockdown is shown in middle. Middle, ED-1 cells overexpressing WT CP110 or an empty vector were transfected with each of two different CP110-targeting siRNAs and control siRNA. Twenty-four hours later, cells were fixed and scored for multipolar anaphases. Right, 24 hours after siRNA transfection, ED-1 cells were treated with indicated seliciclib dosage and scored for multipolar anaphases. B, effect of CP110 overexpression on CDK2 inhibitor activity. Left, confirmation of CDK2 mRNA knockdown by real-time RT-PCR and immunoblot analyses, respectively. Middle, ED-1 cells overexpressing WT CP110 or an empty vector were transfected with two different CDK2-targeting siRNAs and control siRNA and scored for multipolar anaphases 24 hours after transfection. Right, ED-1 cells overexpressing WT CP110 or an empty vector were treated with indicated seliciclib dosages. ED-1 cells were scored for multipolar anaphases, 24 hours later.

KRAS sensitizes cancer cells to anaphase catastrophe by decreasing CP110 levels

To investigate the role of *KRAS* in seliciclib-mediated cytotoxicity, a $KRAS^{G12V}$ expression vector or an empty vector was independently stably transfected into ED-1 cells. Expression of oncogenic *KRAS* was confirmed by immunoblot analyses (Fig. 5A). $KRAS^{G12V}$-transfected ED-1 cells (KRAS-ED-1) exhibited marked growth inhibition (Supplementary Fig. S4A), increased multipolar anaphases (Fig. 5A) and apoptosis (Fig. 5B) after seliciclib treatment as compared with control transfectants. Thus, *KRAS* activation sensitized lung cancer cells to pharmacologic CDK2 inhibition, as is consistent with previous work (5, 7).

CP110 protein levels were downregulated in KRAS-ED-1 cells, but CP110 mRNA levels were not appreciably affected as compared with control cells (Fig. 5C). CP110 protein levels were also lower in 344p, 393p, and LKR13 murine lung cancer cells that harbor activating *KRAS* mutations as compared with ED-1 cells that express WT KRAS (Supplementary Fig. S4C). To further explore the role of *KRAS* in regulating CP110 expression, transient KRAS knockdown was achieved in 344p and Hop62 cells using siRNAs. Decreased KRAS expression was detected at 48 and 72 hours after transfection. Increased CP110 expression was evident 72 hours after transfection for 344p cells and 96 hours after transfection for Hop62 cells (Supplementary Fig. S4D and S4E). This delay in a change in CP110 expression implied that CP110 expression was regulated by targets downstream of *KRAS*.

To learn whether CP110 overexpression could reverse KRAS-ED-1 cells sensitivity to CDK2 inhibition, WT CP110 was overexpressed in them. This reduced both multipolar anaphases and apoptosis (Fig. 5D and E). Therefore, KRAS activation repressed CP110 expression, which enhanced lung cancer cell response to CDK2 inhibition.

CP110 expression in lung cancers

To investigate whether CP110 was differentially expressed in human lung cancers with different *KRAS* mutation status, tumor histology, size, age, or stage CP110 IHC assays were performed (Fig. 6A).

In murine lung cancer cell lines driven by *KRAS* expression (LKR13) or not (ED-1), CP110 levels were 2.6-fold higher in ED-1 than in LKR13 cells (Supplementary Fig. S4C). Immunohistochemical expression profiles were also examined in the normal

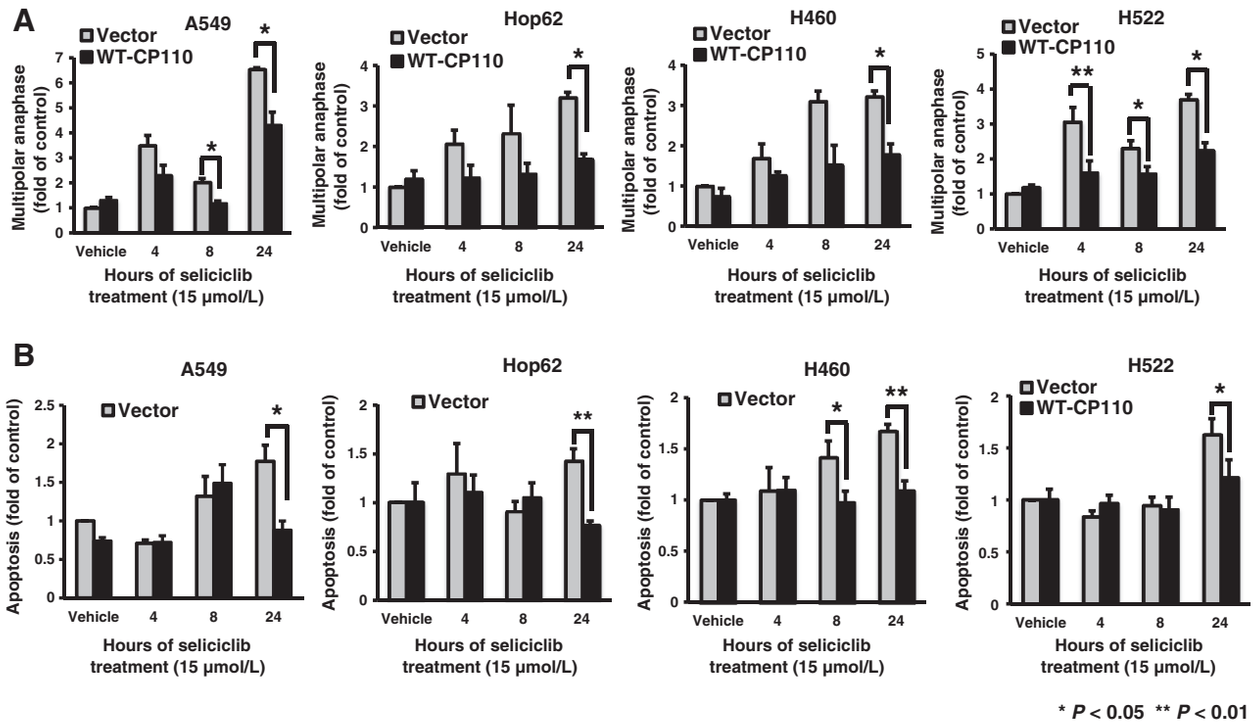

Figure 3.

Overexpression of CP110 rescues anaphase catastrophe induced by CDK2 inhibition in human lung cancer cells. A549, Hop62, H460, and H522 human lung cancer cells overexpressing CP110 were each treated with seliciclib (15 μmol/L) for indicated hours and scored for multipolar anaphase (A) and analyzed for apoptosis (B) as detected by Annexin V:FITC and 7-aminoactinomycin D staining.

versus malignant lung tissues from *KRAS* or cyclin E-driven murine transgenic lung cancers (Supplementary Fig. S5). Notably, the intensity of CP110 staining was much lower in the *KRAS*-driven lung cancers as compared with lung cancers with WT KRAS status.

CP110 expression was higher in human malignant versus adjacent normal lung tissues (Fig. 6A and 6B). A logistic regression model using CP110 intensity as a dichotomous outcome (CP110 intensity $\geq$ 200, median) revealed that a larger proportion of adenocarcinomas with *KRAS* mutations were low CP110 intensity as compared with *KRAS* WT adenocarcinomas (Fig. 6C). However, average CP110 intensity did not show a difference between *KRAS* mutant and WT lung tumors (data not shown). No significant differences were observed in CP110 expression in lung cancer cases when stratified for survival (Fig. 6D), tumor stage or age at diagnosis (data not shown).

Discussion

This study revealed that CP110 expression determines the extent of anaphase catastrophe when CDK2 levels or activity are inhibited. Reducing CP110 levels promotes anaphase catastrophe and overexpression of CP110 significantly reduces anaphase catastrophe conferred by genetic or pharmacologic inhibition of CDK2. Time-lapse live-cell imaging provided direct evidence demonstrating that anaphase catastrophe results in apoptosis in human lung cancer cells.

CP110 interacts with distinct protein complexes that regulate centrosome duplication and separation, chromosome segregation, and cilia formation (16–20). It is not known to have enzymatic activity, but is thought to function structurally to regulate microtubule growth and centriole length (29). CP110 is a direct target of cyclin E-CDK2 (15); however, functional consequences of specific CP110 sites of phosphorylation by CDK2 are not yet known. Studies presented in Fig. 2 revealed that CP110 repression caused anaphase catastrophe. The impact of CP110 on CDK2 inhibition–mediated anaphase catastrophe was studied further.

Intriguingly, engineered *KRAS* expression downregulated CP110 levels in lung cancer cells, which provided an explanation for the observed enhanced sensitivity of lung cancer cells with *KRAS* mutations to CDK2 inhibition (5). *KRAS* mutations are linked to centrosome amplification (30, 31) and chromosomal instability (32). The deregulation of CP110 linked to activated *KRAS* found here likely contributes to these processes.

CP110 is expressed ubiquitously in normal tissues (15). Expression of CP110 changes in the cell cycle and is repressed when cells enter G_0 phase (15). The upregulation of CP110 expression evident in malignant versus normal lung tissues could reflect an increased proliferation of lung cancer cells or the presence of inflammation because proinflammatory cytokines enhance CP110 expression (33).

High CP110 expression induces centrosome amplification (20), but then delays centrosome separation and promotes centrosome clustering. High CP110 expression should protect cancer cells with supernumerary centrosomes from undergoing multipolar cell division. High CP110 expression also inhibits primary cilia formation (18). This contributes to cilia defects in cancer cells (32). Primary cilia are crucial for signaling pathways through

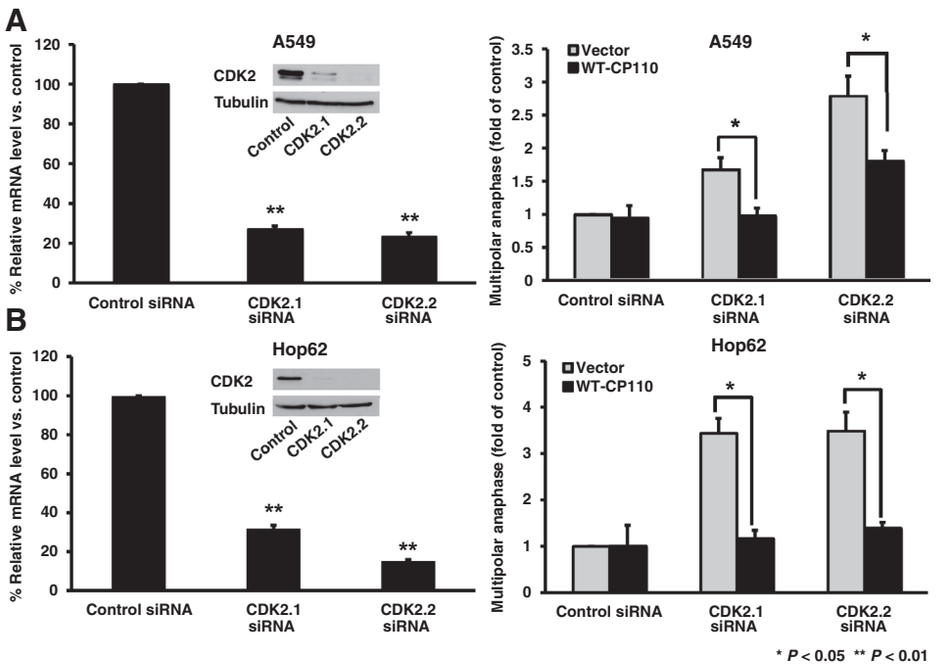

Figure 4.
Overexpression of CP110 rescues anaphase catastrophe caused by genetic CDK2 inhibition in human lung cancer cells. A and B, left, confirmation of CDK2 mRNA knockdown by real-time RT-PCR assays and immunoblots 24 hours after transfection. Right, A549 and Hop62 human lung cancer cells overexpressing CP110 were transfected with siRNA-targeting CDK2 or control siRNA and scored for multipolar anaphase 24 hours after transfection.

PDGFα, Hedgehog, and Wnt, which are essential for growth and differentiation (34, 35). Loss of cilia in cancer cells likely contributes to insensitivity of cancer cells to environmental repressive signals (34). *KRAS* mutations can play a role in primary cilia formation in pancreatic cancers (36). Of note, loss of primary cilia is important in cytogenesis in polycystic kidney disease and seliciclib treatment is reported to block cystogenesis in cultured cells and in mouse models of polycystic kidney disease, but ability to restore primary cilia formation was not examined (37). The relationships between *KRAS* mutation, primary cilia formation, CDK2 inhibition, CP110, and lung carcinogenesis warrant further investigation.

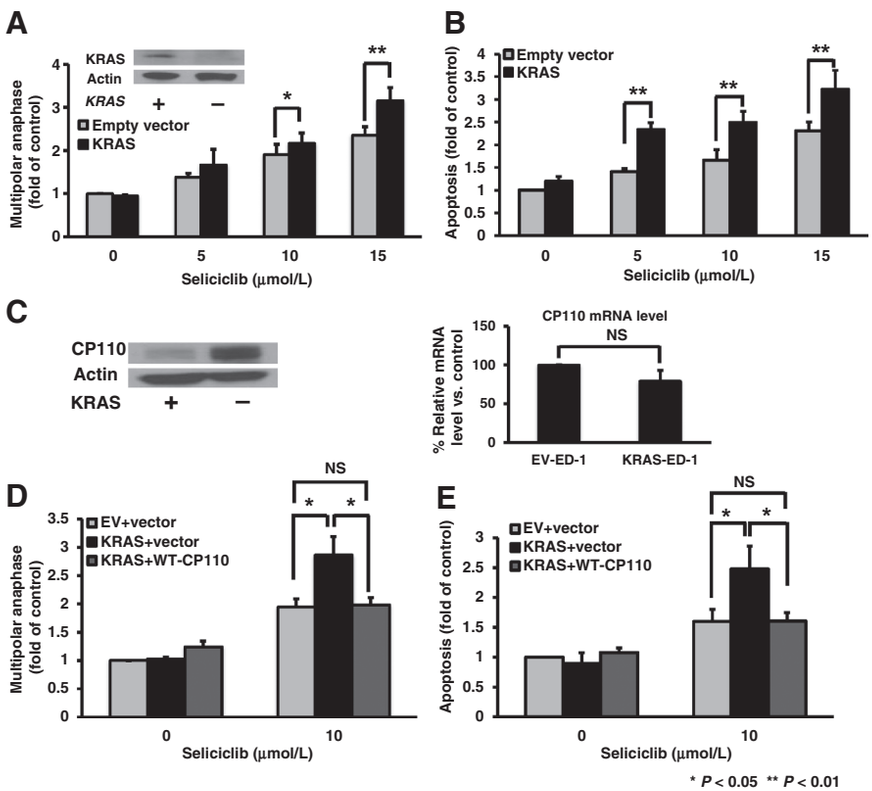

Figure 5.
KRAS mutation affects CDK2 inhibitor activity and deregulates CP110. *KRAS*^{G12V} stably transfected ED-1 cells (*KRAS*-ED-1) showed a marked increase of multipolar anaphase (A) and apoptosis (B) as compared with empty vector–transfected ED-1 cells (EV-ED-1) after 24 hours seliciclib treatment. Increased KRAS protein level was confirmed by immunoblot. C, CP110 expression in *KRAS*-ED-1 cells as compared with EV-ED-1 cells on the protein (left) and mRNA (right) levels. D and E, *KRAS*-ED-1 and empty vector (EV)-ED-1 cells overexpressing WT CP110 were treated with seliciclib (10 μmol/L) for 24 hours and scored for multipolar anaphase (D) and apoptosis (E). NS, not significant.

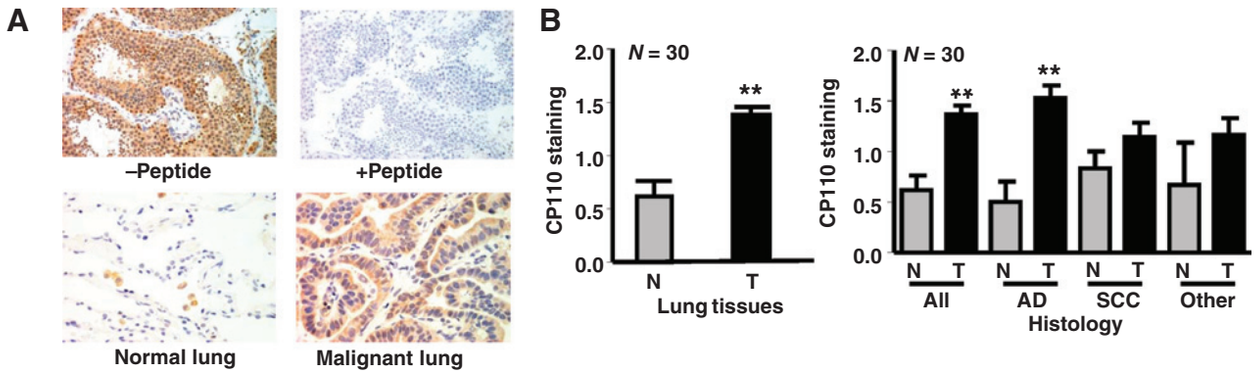

C

Logistic regression model in lung adenocarcinomas using CP110 intensity as a dichotomous outcome

	CP110 intensity < median	CP110 intensity ≥ median	OR	95% CI	*P* value
KRAS WT	118	126	1.0 (ref)	0.36–0.98	0.044
KRAS mutant	54	40	0.59		

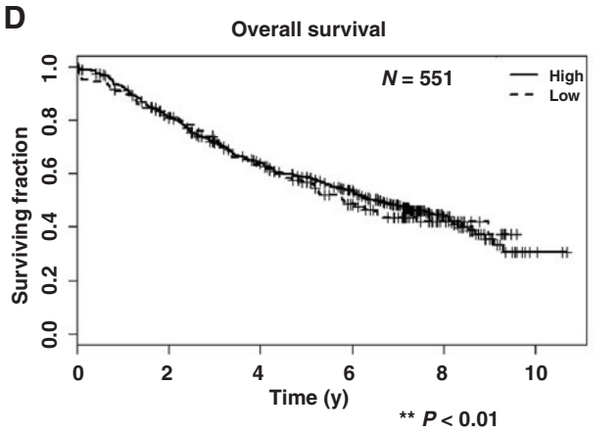

Figure 6.
CP110 expression in human normal versus malignant lung. A, representative CP110 immunostaining of normal adjacent lung versus malignant lung. B, left, quantification of CP110 expression in malignant (T) as compared with normal (N) lung. Right, quantification of CP110 expression in malignant lung versus adjacent normal lung in adenocarcinoma (AD), squamous cell carcinoma (SCC), and other histologic types. C, logistic regression model using CP110 intensity (CP110 intensity $\geq$ 200, median) as a dichotomous outcome comparing KRAS mutant and WT adenocarcinomas. Ref, reference; CI, confidence interval. This model was adjusted for race, gender, tobacco use, and stage. D, the overall survival of CP110 high expressing as compared with CP110 low expressing lung cancer cases.

The biologic relevance of these findings was confirmed in lung cancers from engineered mice where *KRAS* is the driver mutation. These lung cancers exhibited lower CP110 levels as compared with lung cancers from mice with WT *KRAS* (Supplementary Fig. S5). Clinical relevance was established by determining that a larger proportion of lung tumors with *KRAS* mutations were low CP110 expression as compared with *KRAS* WT tumors when using a logistic regression model categorizing tumors into high or low CP110 intensity (Fig. 6C). This finding supports the hypothesis that lung cancers with *KRAS* mutations are likely to be sensitive to a CDK2 inhibitor therapeutic strategy. One of the mechanisms underlying that is low CP110 levels increasing anaphase catastrophe. Although the overall average CP110 levels between *KRAS* mutant and WT lung cancers did not show a significant difference, it is possible that the immunohistochemical assay used was not sufficiently sensitive to appreciate subtle differences in CP110 expression.

The effect of *KRAS* mutations on CP110 expression is likely complex and other proteins that interact with CP110 could be affected by *KRAS* mutations. For instance, CP110 expression is controlled by two independent ubiquitination pathways, $SCF^{cyclinF}$-mediated pathway (20) and NEURL4–HERC2 complex–mediated pathway (38). Recently, a centriolar deubiquitinating enzyme, USP33, was found to regulate CP110 expression by countering cyclin-F–mediated destruction (25).

In summary, this study identified CP110 as a key mediator of anaphase catastrophe induced by CDK2 inhibition that temporally precedes apoptosis. *KRAS* mutations sensitized lung cancer cells to seliciclib-mediated CDK2 inhibition, inducing anaphase catastrophe in part by downregulating CP110 levels. The translational relevance of this finding is underscored by the fact that CP110 is frequently overexpressed in NSCLCs and a larger percentage of lung cancers with *KRAS* mutation are low CP110 expressing. Taken together, these findings indicate a mechanistic link between CP110 expression and *KRAS* mutation. It is proposed that these species are important to prioritize selection of a CDK2 inhibitor for the clinical treatment of *KRAS*-mutant lung cancers.

Disclosure of Potential Conflicts of Interest

No potential conflicts of interest were disclosed.

Authors' Contributions

Conception and design: S. Hu, A.V. Danilov, F. Galimberti, S. Ravi, S. Freemantle, D.A. Compton, E. Dmitrovsky

Development of methodology: S. Hu, A.V. Danilov, L.J. Tafe, B. Mino, V.A. Memoli, F. Galimberti, S. Ravi, A. DeCastro, I.I. Wistuba, S. Freemantle, E. Dmitrovsky
Acquisition of data (provided animals, acquired and managed patients, provided facilities, etc.): S. Hu, K. Godek, B. Orr, L.J. Tafe, J. Rodriguez-Canales, C. Behrens, B. Mino, C.A. Moran, V.A. Memoli, L.M. Mustachio, Y. Lu, D. Sekula, A.S. Andrew, I.I. Wistuba, E. Dmitrovsky
Analysis and interpretation of data (e.g., statistical analysis, biostatistics, computational analysis): S. Hu, A.V. Danilov, K. Godek, L.J. Tafe, B. Mino, V.A. Memoli, L.M. Mustachio, Y. Lu, D. Sekula, A.S. Andrew, S. Freemantle, D.A. Compton, E. Dmitrovsky
Writing, review, and/or revision of the manuscript: S. Hu, A.V. Danilov, K. Godek, B. Orr, L.J. Tafe, V.A. Memoli, F. Galimberti, S. Freemantle, D.A. Compton, E. Dmitrovsky
Administrative, technical, or material support (i.e., reporting or organizing data, constructing databases): S. Hu, J. Rodriguez-Canales, V.A. Memoli, D. Sekula, E. Dmitrovsky
Study supervision: S. Freemantle, D.A. Compton, E. Dmitrovsky
Other (performed some of the early-stage experiments): A. DeCastro

Acknowledgments

The authors thank every member in the Dmitrovsky and Compton laboratories for their helpful consultation. The authors thank DartLab: Immunoassay and Flow Cytometry Shared Resource at the Geisel School of Medicine at Dartmouth for technical help.

Grant Support

This study was supported by National Institutes of Health (NIH) and National Cancer Institute (NCI) grants R01-CA087546 (E. Dmitrovsky and S.J. Freemantle), R01-CA190722 (E. Dmitrovsky and S.J. Freemantle), R37-GM051542 (D. Compton), by a Samuel Waxman Cancer Research Foundation Award (E. Dmitrovsky and D. Compton), by a UT-STARS award (E. Dmitrovsky), by Postdoctoral Fellowship PF-12-031-01-CCG (K. Godek), and by an American Cancer Society Clinical Research Professorship (E. Dmitrovsky) provided by a generous gift from the F.M. Kirby Foundation. Dartmouth's Norris Cotton Cancer Center shared resources were used and were supported in part by NCI grant SP30CA623108.

The costs of publication of this article were defrayed in part by the payment of page charges. This article must therefore be hereby marked *advertisement* in accordance with 18 U.S.C. Section 1734 solely to indicate this fact.

Received May 22, 2014; revised January 26, 2015; accepted February 13, 2015; published OnlineFirst March 25, 2015.

References

1. Freemantle SJ, Liu X, Feng Q, Galimberti F, Blumen S, Sekula D, et al. Cyclin degradation for cancer therapy and chemoprevention. J Cell Biochem 2007;102:869–77.
2. Hwang HC, Clurman BE. Cyclin E in normal and neoplastic cell cycles. Oncogene 2005;24:2776–86.
3. Fukuse T, Hirata T, Naiki H, Hitomi S, Wada H. Prognostic significance of cyclin E overexpression in resected non–small cell lung cancer. Cancer Res 2000;60:242–4.
4. Ma Y, Fiering S, Black C, Liu X, Yuan Z, Memoli VA, et al. Transgenic cyclin E triggers dysplasia and multiple pulmonary adenocarcinomas. Proc Natl Acad Sci USA 2007;104:4089–94.
5. Galimberti F, Thompson SL, Liu X, Li H, Memoli V, Green SR, et al. Targeting the cyclin E-Cdk-2 complex represses lung cancer growth by triggering anaphase catastrophe. Clin Cancer Res 2010;16:109–20.
6. Roberts PJ, Stinchcombe TE. KRAS mutation: should we test for it, and does it matter? J Clin Oncol 2013;31:1112–21.
7. Galimberti F, Thompson SL, Ravi S, Compton DA, Dmitrovsky E. Anaphase catastrophe is a target for cancer therapy. Clin Cancer Res 2011;17:1218–22.
8. Ganem NJ, Godinho SA, Pellman D. A mechanism linking extra centrosomes to chromosomal instability. Nature 2009;460:278–82.
9. Levine DS, Sanchez CA, Rabinovitch PS, Reid BJ. Formation of the tetraploid intermediate is associated with the development of cells with more than four centrioles in the elastase-simian virus 40 tumor antigen transgenic mouse model of pancreatic cancer. Proc Natl Acad Sci U S A 1991;88:6427–31.
10. D'Assoro AB, Barrett SL, Folk C, Negron VC, Boeneman K, Busby R, et al. Amplified centrosomes in breast cancer: a potential indicator of tumor aggressiveness. Breast Cancer Res Treat 2002;75:25–34.
11. Lingle WL, Salisbury JL. Altered centrosome structure is associated with abnormal mitoses in human breast tumors. Am J Pathol 1999;155:1941–51.
12. Pihan GA, Wallace J, Zhou Y, Doxsey SJ. Centrosome abnormalities and chromosome instability occur together in pre-invasive carcinomas. Cancer Res 2003;63:1398–404.
13. Giehl M, Fabarius A, Frank O, Hochhaus A, Hafner M, Hehlmann R, et al. Centrosome aberrations in chronic myeloid leukemia correlate with stage of disease and chromosomal instability. Leukemia 2005;19:1192–7.
14. Kwon M, Godinho SA, Chandhok NS, Ganem NJ, Azioune A, Thery M, et al. Mechanisms to suppress multipolar divisions in cancer cells with extra centrosomes. Genes Dev 2008;22:2189–203.
15. Chen Z, Indjeian VB, McManus M, Wang L, Dynlacht BD. CP110, a cell cycle-dependent CDK substrate, regulates centrosome duplication in human cells. Dev Cell 2002;3:339–50.
16. Schmidt TI, Kleylein-Sohn J, Westendorf J, Le Clech M, Lavoie SB, Stierhof YD, et al. Control of centriole length by CPAP and CP110. Curr Biol 2009;19:1005–11.
17. Tsang WY, Spektor A, Luciano DJ, Indjeian VB, Chen Z, Salisbury JL, et al. CP110 cooperates with two calcium-binding proteins to regulate cytokinesis and genome stability. Mol Biol Cell 2006;17:3423–34.
18. Tsang WY, Bossard C, Khanna H, Peränen J, Swaroop A, Malhotra V, et al. CP110 suppresses primary cilia formation through its interaction with CEP290, a protein deficient in human ciliary disease. Dev Cell 2008;15:187–97.
19. Spektor A, Tsang WY, Khoo D, Dynlacht BD. Cep97 and CP110 suppress a cilia assembly program. Cell 2007;130:678–90.
20. D'Angiolella V, Donato V, Vijayakumar S, Saraf A, Florens L, Washburn MP, et al. SCF (Cyclin F) controls centrosome homeostasis and mitotic fidelity through CP110 degradation. Nature 2010;466:138–42.
21. Le Tourneau C, Faivre S, Laurence V, Delbaldo C, Vera K, Girre V, et al. Phase I evaluation of seliciclib (R-roscovitine), a novel oral cyclin-dependent kinase inhibitor, in patients with advanced malignancies. Eur J Cancer 2010;46:3243–50.
22. Dragnev KH, Ma T, Cyrus J, Galimberti F, Memoli V, Busch AM , et al. Bexarotene plus erlotinib suppress lung carcinogenesis independent of KRAS mutations in two clinical trials and transgenic models. Cancer Prev Res 2011;4:818–28.
23. Wislez M, Fujimoto N, Izzo JG, Hanna AE, Cody DD, Langley RR , et al. High expression of ligands for chemokine receptor CXCR2 in alveolar epithelial neoplasia induced by oncogenic kras. Cancer Res 2006;66:4198–207.
24. Petty WJ, Li N, Biddle A, Bounds R, Nitkin C, Ma Y, et al. A novel retinoic acid receptor beta isoform and retinoid resistance in lung carcinogenesis. J Natl Cancer Inst 2005;97:1645–51.
25. Li J, D'Angiolella V, Seeley ES, Kim S, Kobayashi T, Fu W, et al. USP33 regulates centrosome biogenesis via deubiquitination of the centriolar protein CP110. Nature 2013;495:255–9.
26. To MD, Quigley DA, Mao JH, Rosario RD, Hsu J, Hodgson G, et al. Progressive genomic instability in the FVB/KrasLA2 mouse model of lung cancer. Mol Cancer Res 2011;9:1339–1345.
27. Pitha-Rowe I, Hassel BA, Dmitrovsky E. Involvement of UBE1L in ISG15 conjugation during retinoid-induced differentiation of acute promyelocytic leukemia. J Biol Chem 2004;279:18178–87.

28. Crasta K, Ganem NJ, Dagher R, Lantermann AB, Ivanova EV, Pan Y , et al. DNA breaks and chromosome pulverization from errors in mitosis. Nature 2012;482:53–8.
29. Kobayashi T, Dynlacht BD. Regulating the transition from centriole to basal body. J Cell Biol 2011;193:435–44.
30. Harrison MK, Adon AM, Saavedra HI. The G1 phase Cdks regulate the centrosome cycle and mediate oncogene-dependent centrosome amplification. Cell Div 2011;6:2.
31. Zeng X, Shaikh FY, Harrison MK, Adon AM, Trimboli AJ, Carroll KA, et al. The Ras oncogene signals centrosome amplification in mammary epithelial cells through cyclin D1/Cdk4 and Nek2. Oncogene 2010; 29:5103–12.
32. Castagnola P, Giaretti W. Mutant KRAS, chromosomal instability and prognosis in colorectal cancer. Biochim Biophys Acta 2005;1756: 115–25.
33. Lai Y, Chen B, Shi J, Palmer JN, Kennedy DW, Cohen NA. Inflammation-mediated upregulation of centrosomal protein 110, a negative modulator of ciliogenesis, in patients with chronic rhinosinusitis. J Allergy Clin Immunol 2011;128:1207–1215.
34. Plotnikova OV, Golemis EA, Pugacheva EN. Cell-cycle–dependent ciliogenesis and cancer. Cancer Res 2008;68:2058–61.
35. Michaud EJ, Yoder BK. The primary cilium in cell signaling and cancer. Cancer Res 2006;66:6463–7.
36. Seeley ES, Carrière C, Goetze T, Longnecker DS, Korc M. Pancreatic cancer and precursor pancreatic intraepithelial neoplasia lesions are devoid of primary cilia. Cancer Res 2009;69:422–30.
37. Bukanov NO, Smith LA, Klinger KW, Ledbetter SR, Ibraghimov-Beskrovnaya O. Long-lasting arrest of murine polycystic kidney disease with CDK inhibitor roscovitine. Nature 2006;444: 949–52.
38. Al-Hakim AK, Bashkurov M, Gingras AC, Durocher D, Pelletier L. Interaction proteomics identify NEURL4 and the HECT E3 ligase HERC2 as novel modulators of centrosome architecture. Mol Cell Proteomics 2012;11:M111.014233.